

Date: 6/15/16

## EIC Detector R&D Progress Report

**Project ID:** eRD1

**Project Name:** EIC Calorimeter Development

**Period Reported:** from 1/1/16 to 6/30/16

**Project Leaders:** H.Z. Huang and C. Woody

**Contact Person:** H.Z. Huang

### Collaborators

*S.Boose, J.Haggerty, J.Huang, E.Kistenev, E.Mannel, C.Pinkenbergl,  
S. Stoll and C. Woody*  
(PHENIX Group, BNL Physics Department)

*E. Aschenauer, S. Fazio, A. Kiselev*  
(Spin and EIC Group, BNL Physics Department)

*Y. Fisyak*  
(STAR Group, Physics Department)  
Brookhaven National Laboratory

*F. Yang, L. Zhang and R-Y. Zhu*  
California Institute of Technology

*T. Horn*  
The Catholic University of America and  
Thomas Jefferson National Accelerator Facility

*W. Jacobs, G. Visser and S. Wissink*  
Indiana University

*A. Sickles and V. Loggins*  
University of Illinois at Urbana Champaign

*C. Munoz-Camacho*  
IPN Orsay, France

*S. Heppelmann*  
Pennsylvania State University

*C. Gagliardi*  
Texas A&M University

*R. Esha, H.Z. Huang, Md. Nasim, M. Sergeeva, S. Trentalange, O. Tsai, and  
L. Wen*  
University of California at Los Angeles

*Y. Zhang, H. Chen, C. Li and Z. Tang*  
University of Science and Technology of China

*H. Mkrtychyan*  
Yerevan Physics Institute

## **Abstract**

We report on the progresses made on the Tungsten-Powder/Scintillating Fiber based EM Calorimeter development and on the PbWO<sub>4</sub> crystal calorimeter development. Beam test runs were carried out at FNAL for the sPHENIX EMCal prototype modules and for the High Resolution EMCal prototype modules. The BNL sPHENIX EMCal team will report on the beam test results for the sPHENIX prototype modules with one-D projective geometry made. Their future plan will focus on sPHENIX specific EMCal development and will not request EIC R&D budget this year. The UCLA team will show the beam test results for the high resolution prototype modules. The team requests \$144.25k for FY2017 to continue the R&D development of compact readout scheme. The CUA crystal R&D team has been working under a very limited budget last year. They will report the results of characterization of PWO crystals and the continued development of testing facilities. They request a budget of \$70k for FY2017. The total budget request from the Calorimeter consortium is \$214.25k for FY2017.

**Sub Project: Progress on Tungsten Powder Calorimeter R&D at BNL**  
**Project Leader: C.Woody**

**Past**

**What was planned for this period?**

Our main goal for this R&D period was to build and test the prototypes of the sPHENIX electromagnetic and hadronic calorimeters in the test beam at Fermilab. As described in our previous report, these consisted of an 8x8 array of W/SciFi EMCAL modules and two steel plate scintillating tile hadronic calorimeters (prototypes of the sPHENIX Inner and Outer HCALs). The beam test was planned for the entire month of April at the Fermilab Test Beam Facility (FTFB) and was designed to test the mid rapidity versions of both the EMCAL and HCAL detectors. The test included a mockup of the sPHENIX solenoid magnet that was placed between the Inner and Outer HCALs, as well a full combined readout and LED calibration system for all three calorimeters. This test was closely related to the development of calorimeters for EIC since we expect the sPHENIX detector and its calorimeter system to serve as an initial Day 1 detector at eRHIC.

Half of the EMCAL modules were produced Tungsten Heavy Powder (THP), which is the company that supplies the tungsten powder for all of our calorimeter modules, and half were produced at the University of Illinois at Urbana Champaign (UIUC). The modules are produced differently at these two locations which allowed us to study two different manufacturing techniques. The process used at THP utilizes a centrifuge method to compact the tungsten powder and epoxy, while the process used at UIUC utilizes a vibration table to compact the powder. All of the EMCAL modules used in the prototype were 1D projective that were tapered only in one dimension (nominally the phi direction) and were representative of the mid rapidity ( $|\eta| \sim 0$ ) region of the sPHENIX calorimeter. The tiles in the two HCALs were also arranged to represent the most central rapidity region.

We also planned to continue our study of radiation damage in SiPMs. Our goal for this period was to carry out more measurements with gamma rays and neutrons along with additional tests in the PHENIX IR.

**What was achieved?**

The beam test at Fermilab was completed as planned and a successful test was achieved for the full sPHENIX prototype calorimeter system. The detectors arrived at the FTFB at the end of March and were installed in the test beam area the week of April 3<sup>rd</sup>. Figure 1 shows the full calorimeter setup as it was during the second half of the run. Initially, the EMCAL was tested upstream of this position and placed on a remotely controlled motion table that allowed us to easily move the detector around in the beam for measuring different positions and configurations. In the downstream position, the EMCAL could be moved manually using a custom designed support structure that placed it in front of the Inner HCAL prototype, and also tilting or rotating the detector at various angles. Both HCAL prototypes were placed on a large lifting table that allowed these detectors to be tilted at an angle of  $\pm 4.5$  degrees in the vertical direction in order to study the angular dependence of the full calorimeter system.

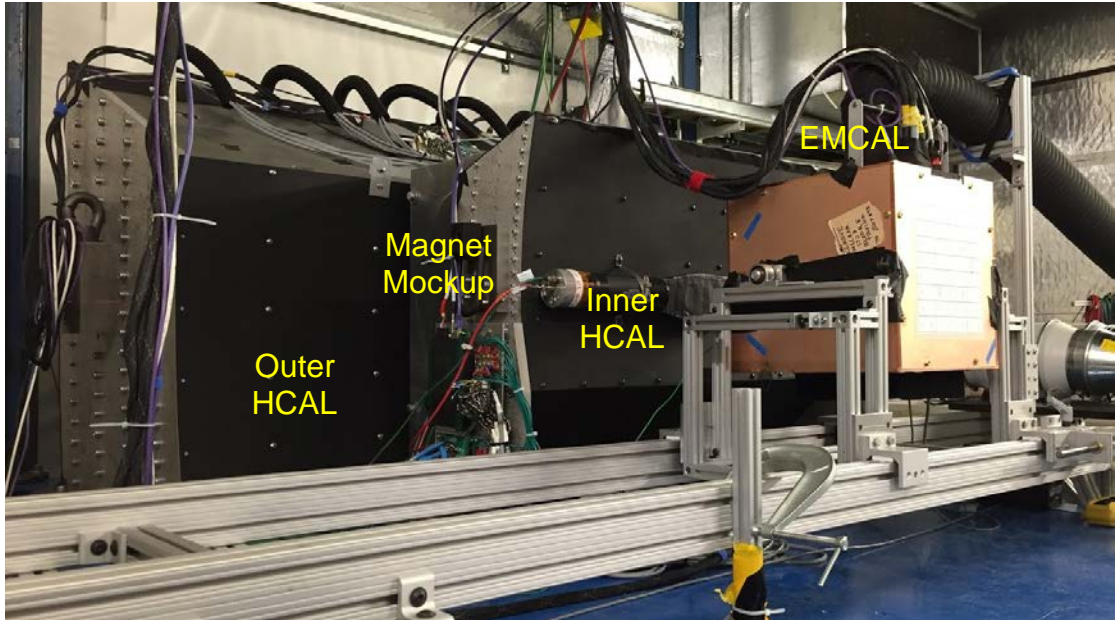


**Figure 1.** All three sPHENIX prototype calorimeters in the downstream position at the Fermilab Test Beam Facility in April 2016. The test setup also included a mock up of the sPHENIX magnet coil and cryostat.

Figure 2 shows the inside of the EMCAL prototype with its 8x8 array of absorber modules along with a map of how the modules from THP and UIUC were arranged. The map also gives the density of each of the modules. In general, the THP modules achieved a higher density, but there is a significant density variation from module to module for both types. This is an area where we plan to put additional effort to improve in the future.



THP 10.2	THP 10.5	THP 8.5	THP 8.5	THP 9.0	THP 9.0	THP 9.8	THP 9.8
THP 9.7	THP 9.7	THP 10.0	THP 10.0	THP 10.0	THP 10.0	THP 9.9	THP 9.9
THP 9.2	THP 9.2	THP 9.8	THP 9.8	THP 9.3	THP 9.3	THP 10.1	THP 10.1
UIUC 9.6	UIUC 9.6	UIUC 9.4	UIUC 9.4	THP 10.1	THP 10.1	THP 9.6	THP 9.6
UIUC 9.5	UIUC 9.5	UIUC 9.5	UIUC 9.5	THP 9.3	THP 9.3	THP 9.3	THP 9.3
UIUC 9.4	UIUC 9.4	UIUC 9.4	UIUC 9.4	UIUC 9.4	UIUC 9.4	UIUC 9.6	UIUC 9.6
UIUC 9.2	UIUC 9.2	UIUC 9.6	UIUC 9.6	UIUC 9.3	UIUC 9.3	UIUC 9.3	UIUC 9.3
UIUC 9.5	UIUC 9.5	UIUC 9.6	UIUC 9.6	UIUC 9.3	UIUC 9.3	UIUC 9.2	UIUC 9.2

**Figure 2.** Inside of the EMCAL prototype showing the 8x8 array of absorber modules. Half of the modules were produced at THP and half at UIUC. The map on the right shows how the modules were arranged inside the detector along with the density of each module.

The EMCAL was first tested in a position further upstream at the FTFB with helium beam pipes along the beamline to minimize interactions of the low energy electron beam. However, there was still significant material in the beam (probably  $\sim 5\% X_0$ ) due to various other detectors and beam instrumentation along the beam line. Each tower was calibrated with minimum ionizing particles using the 120 GeV primary proton beam in order to obtain an initial tower to tower calibration and approximate energy scale for each module. This was done by rotating the detector into the “nose down” position such that the beam passed through eight towers at a time, leaving an energy deposit of  $\sim 30$  MeV in each. Figure 3 shows an example of one of the calibration runs where the beam was passing through the fourth column of towers from the right where a clear MIP peak can be seen.

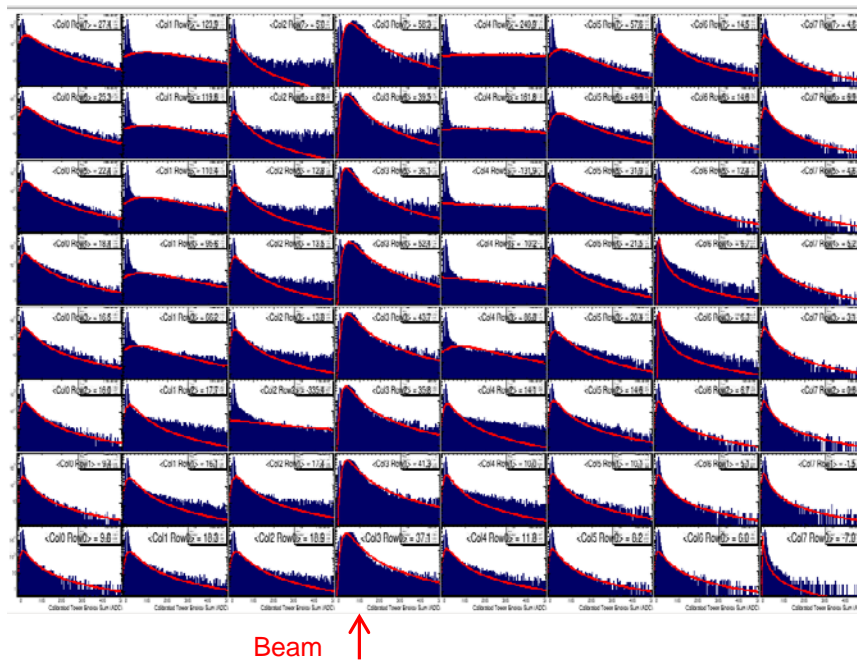


**Figure 3.** MIP calibration of one column of towers in the EMCAL prototype. The detector was placed in the “nose down” position such that the beam passed through eight towers at a time for the MIP calibration runs.

The analysis of the test beam data is still under way, but the first preliminary results for the energy resolution and linearity of the EMCAL prototype look very encouraging. Figures 4 and 5 show the energy resolution and linearity measured over the momentum range from 2 GeV/c to 16 GeV/c for electrons with the beam centered on the UIUC set of modules (the dark blue module in Fig. 2). The upper set of data points in the energy resolution plot were obtained using a MIP calibration for each of the towers while the lower data points were obtained with a tower to tower calibration using electron showers. The electron shower calibration gives an improvement in the statistical term from  $14.2\%\sqrt{E}$  to  $12.7\%/E$  and an improvement in the constant term from 5.4% to 3.2%. Neither set of data have been corrected for the beam momentum spread, which we believe is  $\sim 2\%$  over this energy range. The green curve in Fig. 4 shows the expected resolution from our GEANT4 Monte Carlo simulation of the EMCAL prototype and shows good agreement with the data is. We also verified that the light yield of the modules was  $\sim 500$  p.e./GeV, which agreed well with our expectations.

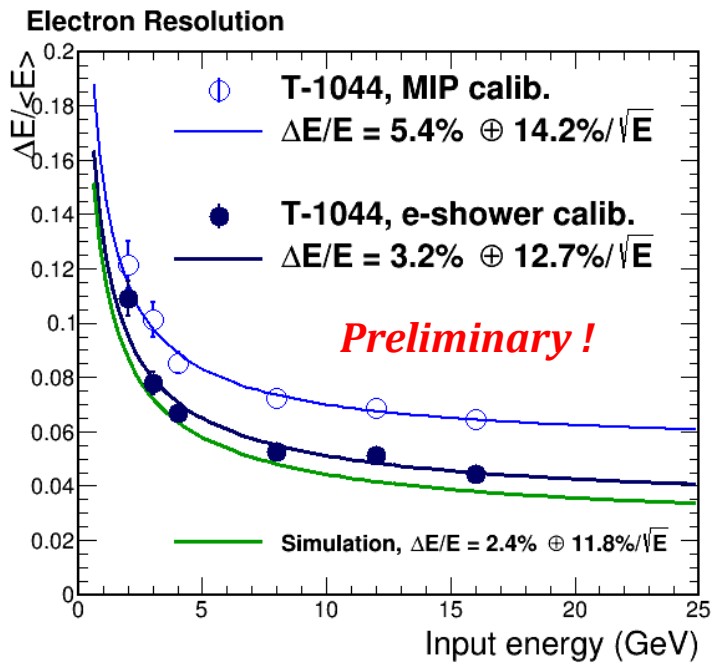


**Figure 4.** Preliminary energy resolution for the EMCAL prototype measured for electrons. The upper data points were computed using a MIP calibration for each tower while the lower data points use a tower to tower calibration using electrons. Neither set of data have been corrected for the beam momentum spread which we believe is  $\sim 2\%$ . The green curve gives our Monte Carlo simulation of the prototype calorimeter.

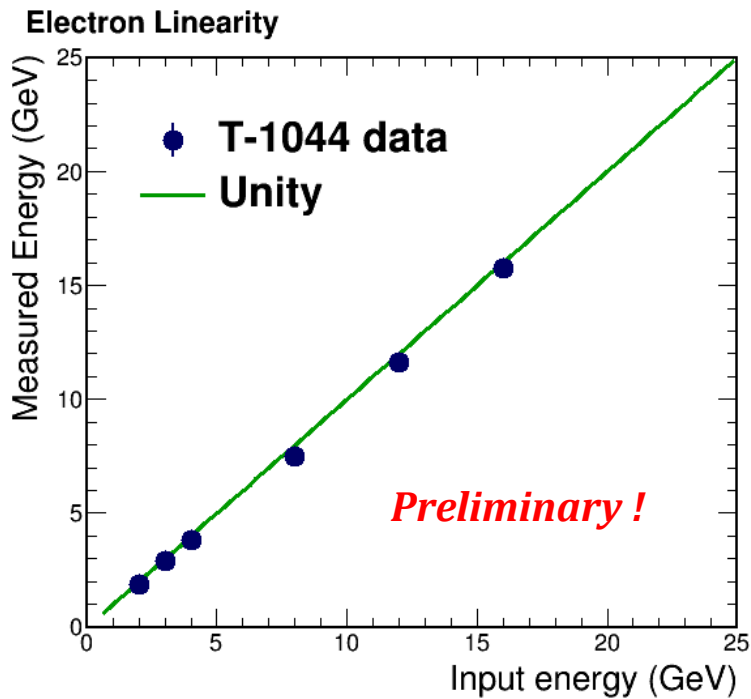


**Figure 5.** Linearity of the EMCAL prototype for electrons from 2-16 GeV/c.

The same GEANT 4 simulation was also used to compare to the results of the eRD1 measurement of similar W/ScFi modules produced at UCLA and measured in the same test beam in 2014. The 4x6 array of 1D projective modules used in that test were simulated using the same GEANT4 program. Figure 6 shows a result of that comparison for electrons and pions at 8 GeV/c. Again, the agreement between the data and simulation is very good.

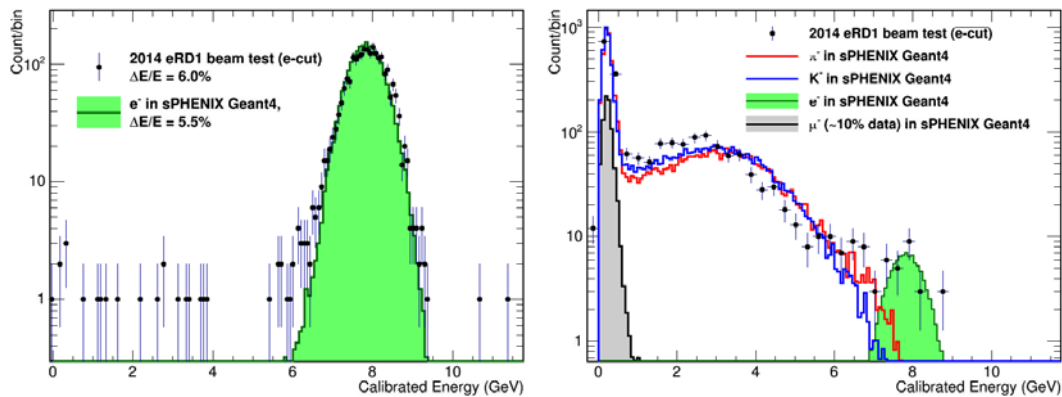


**Figure 6.** Comparison of our GEANT4 Monte Carlo simulation of the 4x 6 array of 1D projective towers built at UCLA and tested at the FTFB in 2014. The left plot is for electrons and the right plot is for pions, both at 8 GeV/c.

### What was not achieved, why not, and what will be done to correct?

The beam test at Fermilab was very successful and we achieved essentially all of our original goals. A complete series of measurements was carried out to study the EMCAL prototype, including its energy resolution, linearity, angular dependence, uniformity across the modules, light yield for electron showers, a study of Cherenkov light produced in the light guides, and much more. Data was also taken with the EMCAL rotated by 45 degrees with respect to the incoming beam to study how the 1D projective modules would perform at larger rapidities. In addition, a combined test of the EMCAL prototype with the two sPHENIX hadronic calorimeter prototypes was also carried out in order to study the combined hadronic energy resolution, linearity,  $e/\pi$  ratio, etc. A full readout and calibration system of the combined calorimeters was also tested. Of course, there are always additional measurements that one would like to have performed had time permitted, but we successfully completed all of the main tests we had originally planned.

We did not achieve the overall average density for the modules that we had hoped, and there was more variation in the density from module to module than we can ultimately accept. This was true for both the THP and UIC modules. We plan to work on improving this during the next R&D period by ensuring better process and quality control in fabricating the modules. The modules also showed some variation in the fiber spacing at the narrow end of the modules, which was due to the fibers not being well supported at this end during the casting process. This problem is relatively easy to fix by adding an additional mesh beyond the last one that is currently used. This procedure was tested at UIUC after the last modules for the prototype were produced and it seemed to work very well.

We also did not make much progress on the development of the 2D projective modules since our priorities were focused on completing the 1D projective EMCAL prototype and testing it during the beam test. Now that that test is complete, we plan

to focus more on this during the next R&D period. However, this will be done as part of our sPHENIX R&D program and is included as part of our EIC R&D.

We also did not manage to carry out more radiation damage tests with SiPMs. This again was simply due to lack of time and having a higher priority for the beam test. However, we did identify a new group of collaborators on this effort, which is the group at Debrecen University in Hungary. They have expertise with SiPMs and also excellent facilities to perform some of the irradiations at their affiliated institution, Atomki, in Debrecen. In addition, we are now collaborating with BNL's Instrumentation Division and Stony Brook to study radiation damage and materials properties in SiPMs as part of an LDRD proposal.

## **Future**

### **What is planned for the next funding cycle and beyond? How, if at all, is this planning different from the original plan?**

Our main activity during the next six months will be analyse the test beam data and produce a publication of the final results. This will include not only the EMCAL, which is the main focus of our EIC R&D, but also the HCAL in order to have a complete set of results for the sPHENIX calorimeters. A great deal of data was taken and the analysis will involve a number of institutions within sPHENIX, many of which are also part of the EIC R&D effort.

We also plan to try and improve the production of the 1D projective modules, both at THP and UIUC. We now have an SBIR with THP that will support this effort, and the work at UIUC will be supported by sPHENIX. We also plan to pursue our development of the 2D projective modules. This effort will take place at UIUC and BNL.

We plan to carry out another beam test at Fermilab early next year to study the three sPHENIX calorimeters at larger rapidity. This will involve making new presumably 2D projective modules for the EMCAL and installing new tiles in the two HCAL prototypes for the larger eta configuration. We plan to repeat many of the same studies we did during the April beam test along with new studies that will involve different possible configurations. Additional Monte Carlo simulations will also be carried out to study these various configurations.

We also plan to continue our tests of radiation damage in SiPMs as described above. These will involve measurements with neutrons and gamma rays at BNL and with our collaborating institutions in Debrecen Hungary.

### **What are critical issues?**

The most critical issue for sPHENIX during the next six months is to measure the calorimeter performance at larger rapidities. This will be done during the beam test early next year. A critical issue for the EMCAL is to measure the performance of the 2D projective modules at large rapidity and compare them to the performance of the 1D modules at large rapidity using the data taken during the April beam test. This comparison will help us decide which way to proceed for the final sPHENIX EMCAL design, which we expect will take place after the 2017 test beam run.

As we have said many times, another critical issue for EIC is how the SiPMs will perform and survive in the radiation environment at EIC. This is an ongoing study that involves both measurements, which we plan to carry out during the next R&D period, as well as more simulations. The recent calculation presented at the last R&D Committee Meeting made good progress along this direction, but further improvements in the simulations are required to better understand what the actual radiation environment will be. This also involves a better model of what the EIC machine design will look like, particularly in the vicinity of the IR where the detector will be located.

## **Manpower**

*Include a list of the existing manpower and what approximate fraction each has spent on the project. If students and/or postdocs were funded through the R&D, please state where they were located, what fraction of their time they spend on EIC R&D, and who supervised their work.*

There are no changes to the official list of EIC calorimeter R&D collaborators since the last report, although there are many institutions collaborating on developing the sPHENIX calorimeters that contribute in a significant way to our EIC calorimeter R&D effort.

## **External Funding**

*Describe what external funding was obtained, if any. The report must clarify what has been accomplished with the EIC R&D funds and what came as a contribution from potential collaborators.*

The R&D on the sPHENIX calorimeters is being supported mostly by sPHENIX R&D funds. In particular, this includes the development of the 2D projective modules which are not required for EIC, but would be a part of the sPHENIX EMCAL if that option is adopted and would then be used at EIC if sPHENIX becomes a Day 1 Detector for eRHIC. Future work at THP on 1D or 2D projective modules will be supported by the newly awarded SBIR that we now have with them. The work on studying radiation damage in SiPMs is partly funded by PHENIX and partly through the LDRD we have with BNLs Instrumentation Division to study SiPMs in extreme environments (high radiation and low temperatures). As a result, we do not require additional support from EIC funds for the next Fiscal Year.

## **Publications**

*Please provide a list of publications coming out of the R&D effort.*

Preliminary results of the recent sPHENIX beam test was presented at the CALOR 2016 Conference in Daegu, Korea in May 2016, and these results will be published in the proceedings of that conference which will be submitted in June 2016. Another contribution was submitted to the 2016 IEEE NSS/MIC conference that will take place in Strasbourg, France in November 2016, and we plan to submit a complete publication of the test beam results to the IEEE Transactions on Nuclear Science.

**Sub Project: Progress on Tungsten Powder Calorimeter R&D at UCLA**  
**Project Leader: H.Z. Huang and O. Tsai**

**What was planned for this period?**

- Build High Resolution (HR) BEMC prototype with square fibers.
- Perform decisive test of two BEMC high-resolution (HR) prototypes at FNAL.
- Perform measurements at RHIC with FEMC to search for possible anomalous signals when using SiPM read-out.

**What was achieved?**

We achieved most of the goals we planned for the past 12 months. Based on results of tests at FNAL and RHIC we have identified future high priority directions in our development of sampling calorimeters for EIC. Detailed studies of two High Resolution (HR) prototypes demonstrate the excellent capabilities of W-powder ScFi technology for HR sampling calorimetry. The first measurements with silicon readout of the FEMC at RHIC, where environmental conditions are somewhat close to those expected at the EIC, revealed unexpected behaviour associated with SiPMs, which will require further investigations.

**High Resolution Sampling Calorimeters for EIC**

For the outgoing electron direction at the EIC, we envision a forward EM calorimeter consisted of two parts: a central region (impact angles of less than 10 degrees) of very high resolution ( $2\%/\sqrt{E}$ ) crystal (PWO) and a peripheral part with a high resolution ( $\sim 7\%/\sqrt{E}$ ) sampling calorimeter.

The first construction of such a sampling calorimeter was made last year (2015) and a prototype was tested at FNAL for a high sampling frequency EMCAL, which has composite absorber made of mixture of W and Sn powders. The readout for this detector was a straight copy of the readout we developed for the BEMC a year earlier. As we reported last year, the targeted energy resolution was not reached (measured  $\sim 10\%/\sqrt{E}$ ) and the reasons why it was not reached were not completely clear. We identified a few potential problems with the first HR prototype: homogeneity of the composite absorber, consistency of the sampling frequency with thin fibers, potential damage at the end of the fibers due to machining through the absorber, light yield from thin fibers and efficiency of light collection with compact readout. This 'old' prototype was then re-worked in order to reduce the number of uncertain factors affecting the energy resolution of the detector. We effectively eliminated all factors except the homogeneity of the composite absorber and consistency of sampling frequency. Both of these contribute to the uniformity of the sampling fraction inside the detector, but quantifying the impact from these two effects would require completely destructive test of this prototype. To decisively answer the question '**is this technology still feasible towards high-resolution calorimeters with future development?**' we proposed to build an additional prototype which did not have complications with the homogeneity of absorber and consistency of sampling frequency. This prototype consisted of thicker, square fibers and an absorber of 100% W-powder. The mechanical parameters of both Old ("O") and New ("N") detectors are listed in Table 1.

Detector	Fibers SCSF 78	Absorber	Sampling Frequency	Composition by weight	Number of fibers in superblock
“Old” High sampling frequency	Round, 0.4mm	75% W 25% Sn	0.671 mm Staggered Pattern	W -0.665 Sn - 0.222 Sc - 0.057 Epoxy- 0.056	25112 Damaged 3
“Square” High sampling fraction	Square, 0.59 x 0.59 mm <sup>2</sup>	100% W	0.904 mm Square Pattern	W - 0.858 Sc- 0.075 Epoxy- 0.067	11664 Damaged 0

The sizes of both HR prototypes were significantly larger, compared to our previous detectors due to increased sampling fraction. Figure 1 shows the HR prototypes next to the FEMC and CEMC modules which were tested in previous years.



**Figure 1: HR prototypes for EIC.**

The ‘O’ detector is about 19 X<sub>0</sub> long compare to the 20X<sub>0</sub> ‘S’ detector. Some length in the ‘O’ detector was lost during re-machining of both front and back sides of the detector. Each HR detector was glued from four individual blocks each about 5 x 5 x 25 cm<sup>3</sup>. The increased size of the HR detectors required us to design and build a new packing machine to keep the sampling fraction constant (+/- 0.2% weight deviation of individual construction blocks). Identical light guides were used to collect light from the HR detectors. During the test run at FNAL we used the same calibrated PMT to read out both HR prototypes, one at a time, in order to compare their performances.

Square scintillation fibers have some attractive properties for an HR type detector: better light yield (according to Kuraray ~ 30% better trapping efficiency compared to round fibers), internal structure of the detector can be made more homogeneous, and it is easier to preserve the sampling fraction and frequency within and between superblocks (glued from four production blocks). In addition, they have a larger surface area for a given volume, which may result in more efficient sampling of the softest shower particles, as was stated by R. Wigman, but to our knowledge which has not been verified experimentally. There are also drawbacks: square fibers are more expensive due to a more ‘difficult’ manufacturing process, the process of stacking them through a set of screens is a bit more labour intensive and they are seemingly, more prone to damage (cracking) to the cladding during stacking through the set of screens, although this may be due to the increased thickness of the fibers. In our previous experience with thin square fibers, we did not notice damage of this type.

The square fibers used for production of the 'S' HR prototype are quite rigid. The straightness of these fibers as delivered is very good. Dimensional tolerances have not been checked on a large sample of fibers due to lack of time (fibers were delivered less than a month before the test run), however our request to change the nominal dimension from 0.6 mm to 0.59 mm for final production was accepted by Kuraray and we confirmed that the central value is indeed 0.59 mm on a small number of fibers from the final production. Figure 2 shows a square fiber assembly in the molding form prior to filling with W powder. Thicker square fibers allow for a very uniform sampling frequency inside the production block.

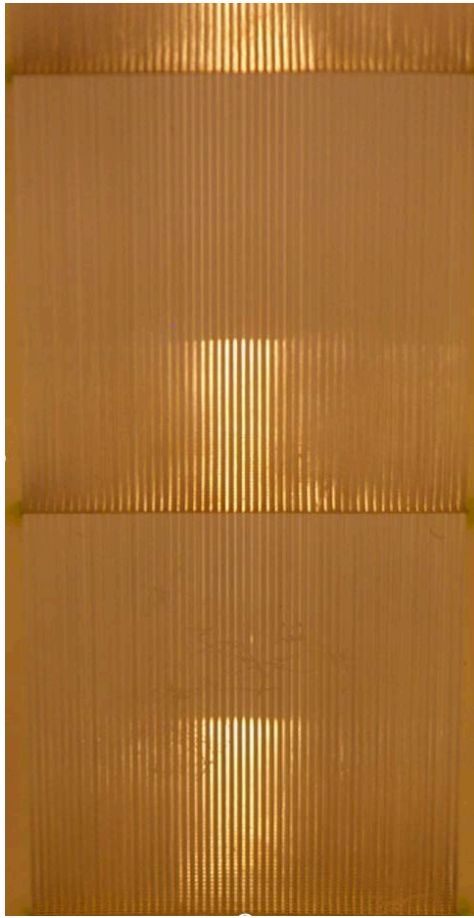


**Figure 2: Square fiber assembly in the molding form.**

As was discussed in our earlier proposal and reports, imperfections in the mechanical structure of the superblock can lead to an increased constant term in the energy resolution of the detector. Any dead area within a production block, between production blocks in the superblock assembly and between superblocks in the final detector assembly will lead to degradation of the energy resolution. This is especially critical to very high density calorimeters we tested in the past. Due to their increased sampling fractions, HR calorimeters should be less prone to such effects, however, higher energy resolution demands strict

requirements on mechanical imperfections. Mechanical imperfections are always a challenge for any calorimeters built from individual blocks. For example, in the nominal mechanical structure of the 'S' prototype the thickness of absorber (distance from the surface of the fibers to the surface of the block) on the sides of the production block is only about 100 microns, which is not trivial to achieve in practice. This is an important consideration, which we will discuss later.

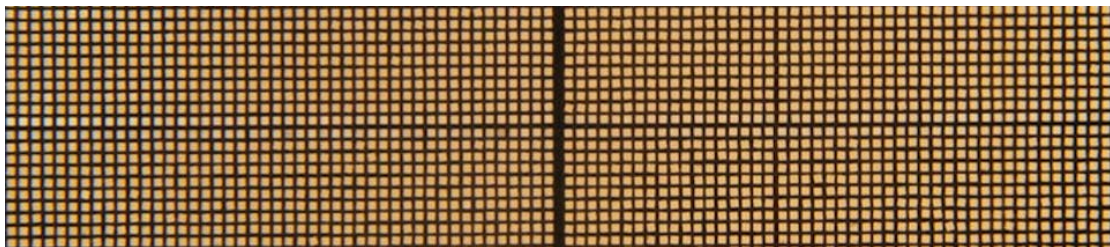


**Figure 3: Mechanical imperfections in the 'S' prototype.**

The Superblock was glued in two steps. First, we glued two doublets and then the two doublets were glued together. Figure 3 shows how well the spacing between the fibers was preserved in doublets, visible as a slightly thicker horizontal black line in the middle of the figure. A thicker, vertical 'dead' area is formed when doublets were glued together or was formed during production of the individual blocks. The expectation was

that this dead area would be about 200 microns thicker than nominal (due to current design of the meshes), however it looks more like 400 microns thicker than nominal. We have some ideas how that may happen, but it is not completely clear at what stage during production this occurred and how this extra dead layer was formed.

### **Results of the Test Run at FNAL (May 4 – May 11, 2016)**

A decisive test should provide answers to these questions:

- Is production homogeneity of the blocks (+- 0.2%) sufficient?
- Are local density/composition variations under control? (Especially for the W/Sn composite absorber during packing.)
- Is the light yield sufficient to allow for compact readout with Si sensors in the future?
- What is the effect of the ‘dead’ areas within and between super-blocks?
- What are benefits of using square fibers?

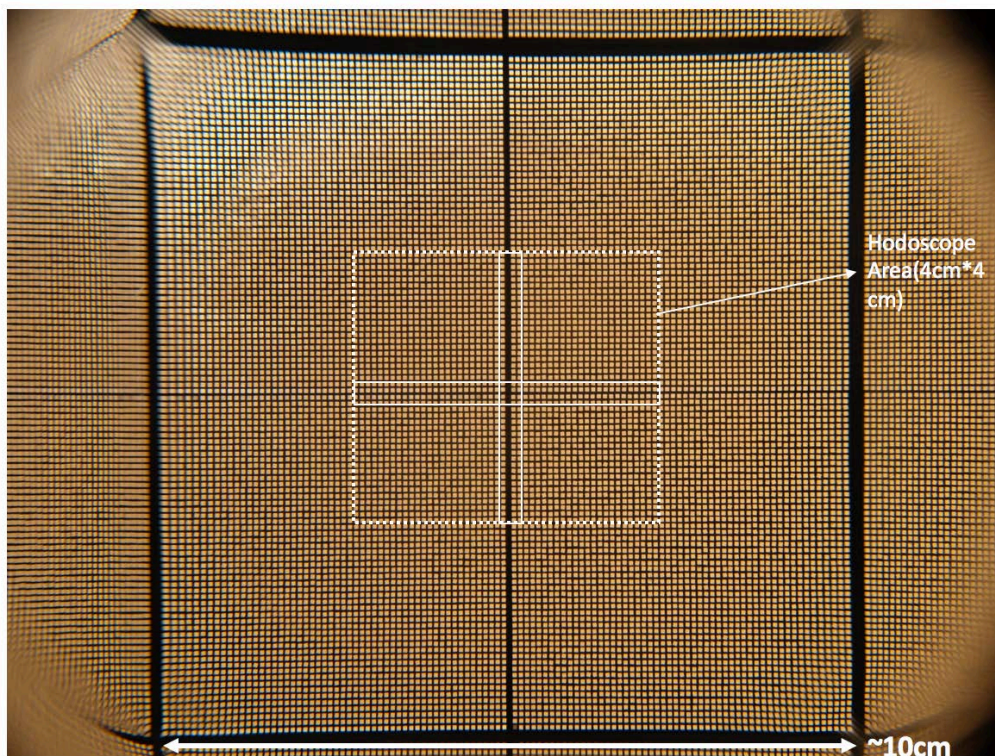


**Figure 4: Selection of impact hits using a Scintillator Hodoscope during the test run. This view of the ‘S’ detector is through the light guide.**

In order to quantify the effect of construction imperfections, we tested a worst-case scenario with the beam centered right in the middle of the superblock, thus sampling both vertical and horizontal dead areas. The beam incident angle was 10 degrees (minimal angle for the BEMC), unless noted otherwise. The cross in the middle of the superblock shows the size of the scintillation hodoscope fingers. The FTBF beam momentum spread of approximately 1.8% for this year’s running conditions was estimated with a beam energy scan on a PbGf block. This number was discussed and found to be consistent with result reported by M. Backfish (FNAL) accelerator physicist responsible for FTBF beam line and L. Bellantoni (FNAL, MINERvA) who did studies

earlier this year on the effect of collimation on dp/p for this beamline (MC, and TOF MINERvA data). The resolution of this standard FTBF PbGI in the test run 16 is consistent with our previous measurements in 2014 and 2015. The accuracy of the beam energy setting was estimated using our data from three independent beam energy scans for the EIC prototypes and discussed with M. Backfish (FNAL) and found to be consistent with his estimates. To extract the energy resolution, the electron peak was fitted within  $\pm 5$  sigma of the mean, except for the 1 and 2 GeV points where the fitting range was restricted from  $-2 + 5$  sigma. The fitting range at low energy was guided by MC and related to radiative losses of the beam upstream of the detector. In total we performed three beam energy scans with the ‘S’ detector, one beam energy scan with ‘O’ detector and one with FTBF PbGI. High statistics data sets were taken at 4 GeV to map the uniformity across the face of the ‘S’ and ‘O’ detectors. Full analysis notes were released to the EIC R&D consortium at the end of the test run and can be found at <https://wiki.bnl.gov/eic/index.php/RD-Calo-2016-05-11#Agenda>

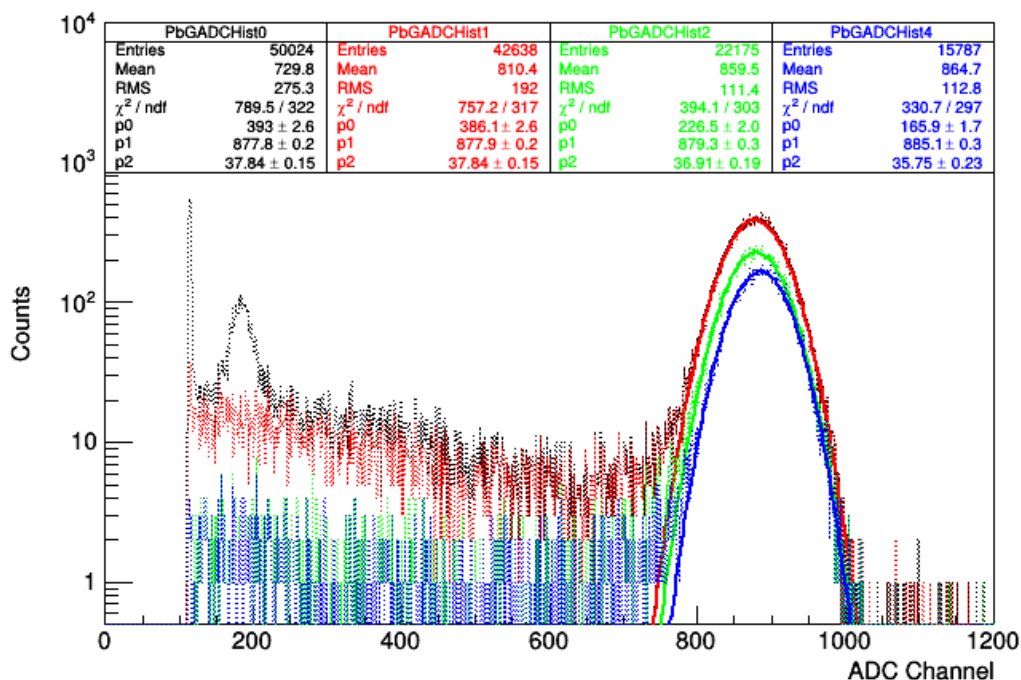


**Figure 5: Typical amplitude spectra for the ‘S’ detector at a beam energy of 3 GeV. Colors correspond to different analysis cuts: Black – raw data, Red +Cherenkov, Green +one hit in Hodoscope, Blue + ‘Geom’ cut.**

The energy resolutions of the ‘S’ and ‘O’ type detectors with a minimal set of cuts (no ‘Geom’ cut) are compared side-by-side in Fig. 6 (‘S’ in the left panel and ‘O’ in the right panel). In both cases, a minimal set of cuts has been used in the analysis. The ‘S’ detector has much better energy resolution, in particular, the constant term in energy resolution is 70% better for the new HR prototype. Both detectors have sufficiently high light yield with an ESR reflector on the front side, giving 5000 p.e./GeV and 3500 p.e./GeV for ‘S’ and ‘O’ detectors, respectively. With a white diffuser reflector on the front side, the ‘S’ detector yields only 3400 p.e./GeV. These numbers need to be corrected to account for losses due to the thin air gap coupling between the light guide and PMT used in the test run, *i.e.*, the light yield is probably a bit higher. More precise estimates of this will be done in near future. These preliminary results indicate that

square fibers produce about 10% more light compared to round fibers for the same weight fraction of scintillator inside the blocks. Future analysis will use Monte Carlo data to correctly account for light yield vs sampling fraction vs shape of fibers used for the ‘S’ and ‘O’ detectors.

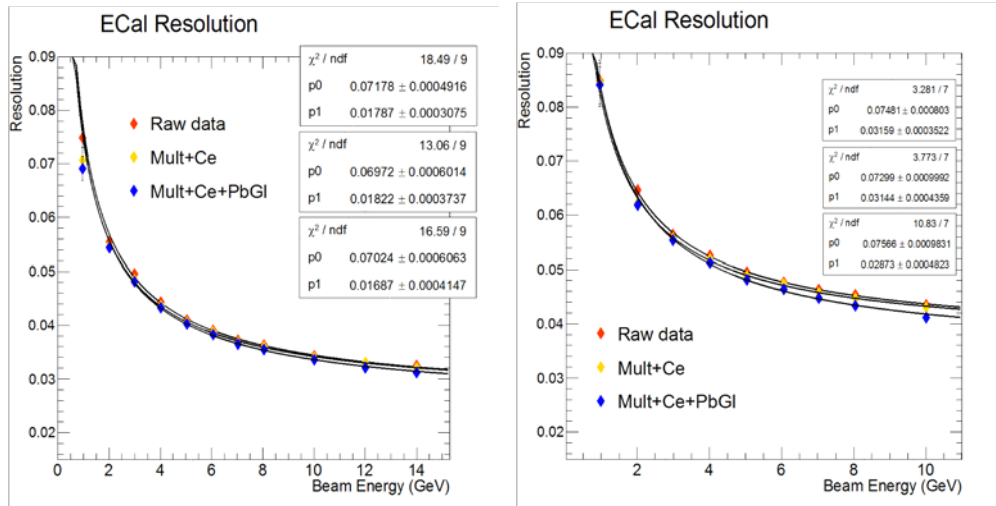


Figure 6: Energy resolution of ‘S’ (left panel) and ‘O’ (right panel) detectors with minimal set of cuts.

To investigate the origin of the constant term, we performed a series of measurements. The first was a high statistic map of the uniformity of response of the detector with the 4 GeV beam. The ‘S’ detector was measured at a nominal position with the wide dead area gap in a vertical orientation as shown in Fig. 4 and then the ‘S’ detector was flipped 90 degrees, so that this gap become horizontal. In the first case, the narrow core of the electromagnetic shower samples this dead area, *i.e.*, crosses the plane of the dead area, while in the second case it is lying in that plane. One can consider these two orientations as the dead area being **non-projective** and **projective**.

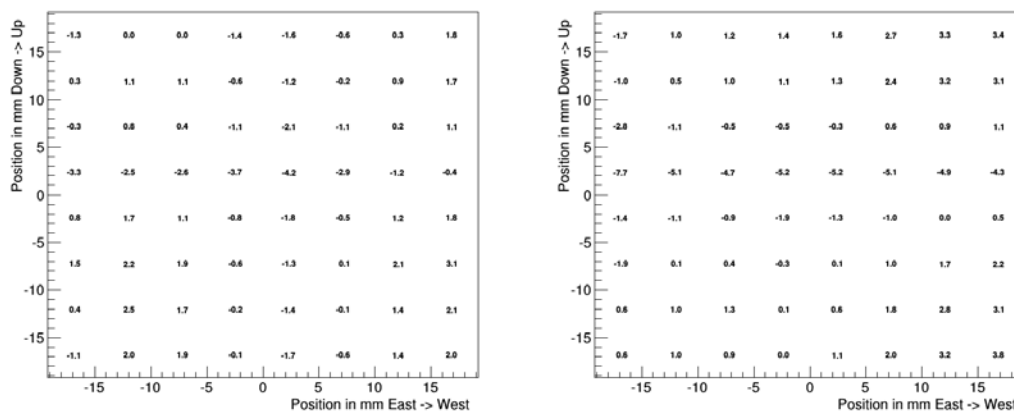
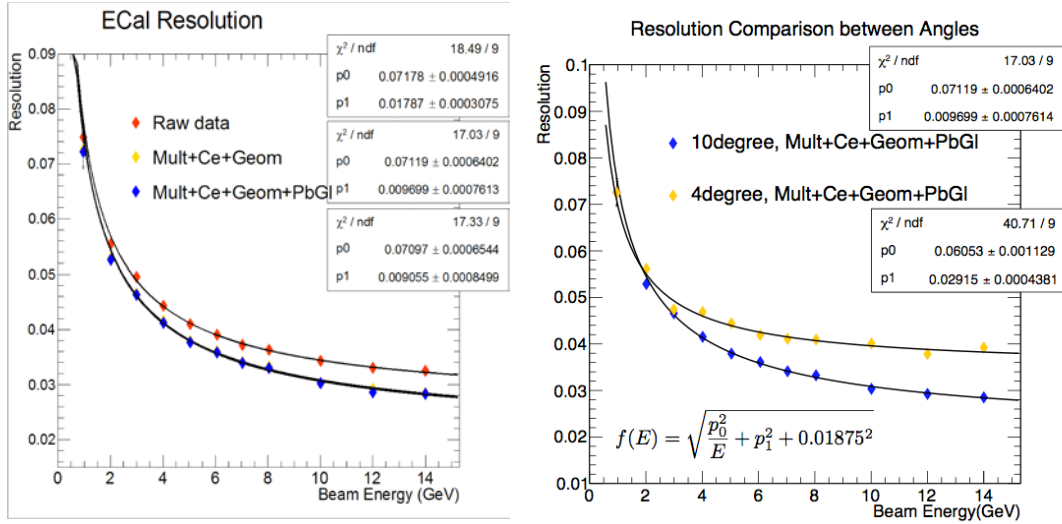


Figure 7: Uniformity of response (in %) for non-projective (right panel) and projective orientation of the dead layer in the ‘S’ detector.

The non-projective orientation of the dead layer created a much smaller (~ factor of two) dip near the dead layer compared to projective placement of dead layer. The RMS in both cases are 1.6% and 2.8%, and the first number is comparable with the constant term in energy resolution shown in Fig. 6 (right panel). If we exclude incoming hits in

areas  $\pm 2.5$  mm around the dead layers, as shown in Fig. 4, the resolution obviously improves and the constant term become less than 1%. This indicates that the internal homogeneity of the ‘S’ type production blocks is very good. (There were concerns prior to the test run that with the significantly increased size and mass of the production blocks compared to our previous detectors we may have had problems with packing W powder, bending fibers etc.) The energy resolution with a stricter ‘Geom’ cut is shown in Fig. 8 (left panel).

The next question we investigated is how much the non-projective orientation of such dead layers should be. All EIC sampling calorimeters envisioned so far will be made from blocks. For the FEMC and CEMC we strongly advocated for non-projective geometry, and all our prototypes for these detectors were non-projective. But in the past two R&D meetings we also heard about projective geometries being pursued. We tested the ‘S’ detector at an impact angle of 4 degrees and compared this with the nominal 10 degree test. The result is shown in Fig. 8 (right panel).



**Figure 8: Energy resolution of the ‘S’ detector with ‘Geom’ cut (left panel). Comparison of the energy resolution of the ‘S’ detector oriented at 4 and 10 degrees (right panel).**

A projective design will result in **unavoidable projective dead layers** between and within calorimeter blocks which will put tough requirements on mechanical tolerances, as discussed in the very first RD1 proposal. Figure 8 (right panel) clearly shows the price one will pay in the projective case with relatively small mechanical imperfections.

A similar analysis was made for the ‘O’ prototype. With the same ‘Geom’ cut used for ‘S’ detector, the constant term is about 2.6%, which is 2.8 times larger than that for the ‘S’ detector. The only explanation for this is that the combination of composite absorber and thin fibers does prevented us from keeping the sampling fraction within production blocks sufficiently uniform. As explained above, all other factors, which could ruin the energy resolution of the ‘O’ detector, were eliminated in the re-worked detector.

To summarize, the test results for the ‘S’ detector are very promising. The uniformity and energy resolution of this detector are already slightly better than that of the excellent H1 ECal. Improvements need to be made to reduce the dead layer between doublets. Contributions to the constant term from mechanical imperfections must be kept as small as possible, because there will be additional contributions to this constant term in the future from compact readout and calibrations. While the light yield seems to be

sufficient for a compact readout with Si sensors, there may be further complications which will be discussed next.

### Tests of FEMC at RHIC during Run16

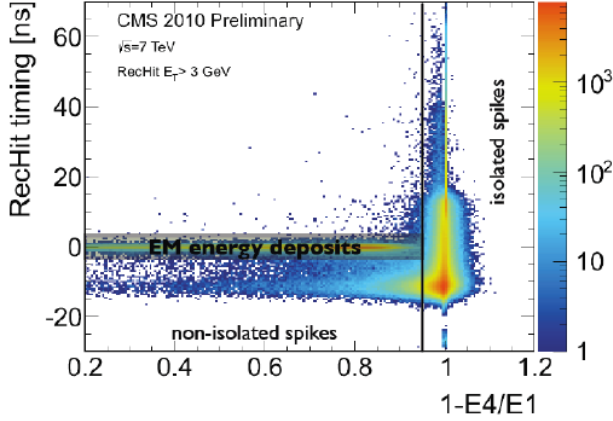


**Figure 9. CMS Anomalous signals.**

These tests were intended to address reports of unexpectedly large fraction of anomalous signals in APDs due to the nuclear counting effect (NCE) observed at CMS at the start of data taking at the LHC with the CMS PWO<sub>4</sub> EMCal as shown in Figure 9.

Additionally, there were reports that SiPMs may not be completely immune to NCEs. To investigate how Si sensor behaves under ‘realistic’ experimental conditions, we equipped the

FEMC with a dual readout. On one side, light from the FEMC was detected by 64 SiPMs (16 towers, 4 SiPM per tower), on the other side of the FEMC, the light was detected by a single large area PMT. We assume that both types of photodetectors will see the same amount of light from each side of the FEMC. Triggering was done on four central channels of the FEMC equipped with SiPMs during the AuAu portion of the run and with APDs during the dAu portion of the run.

The FEMC was located on the East side of the STAR detector, about 1.5 meters from the beam pipe. We present here the preliminary results.

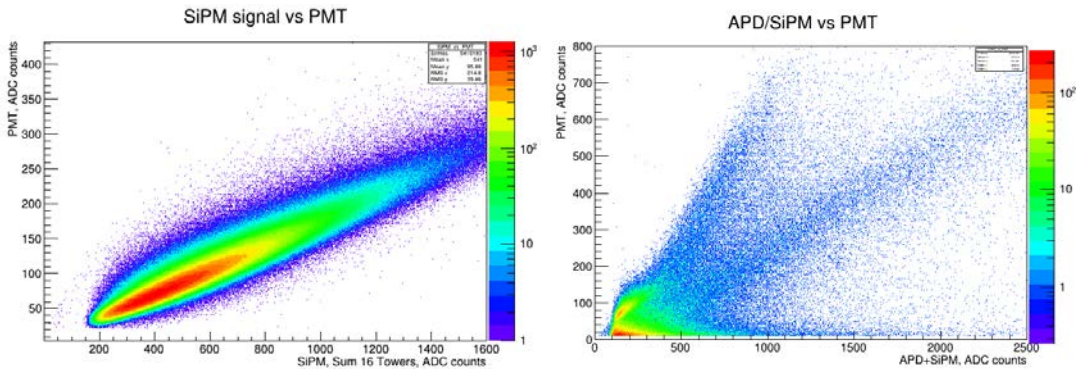


**Figure 10. Correlation between PMT and Si sensors (Sum 16 towers) signals.**

In the case of all SiPM readout we see reasonable correlations between SiPMs and PMT signals, which we discuss in more detail, later. In case of triggering with APDs we see three bands, one is due to NCEs, *i.e.* large signals in the APDs are correlated with very small amplitude signals in the PMT. The origin of the two other bands are not completely clear as of June 2016. Some instrumental effects need to be checked in the lab, for example, the light collection scheme for the APDs was not optimized and

calibration for the APD channels was performed using an LED-monitoring system. The SiPM readout for four channels was replaced with APDs (FEEs were made at IUCF) during the run.

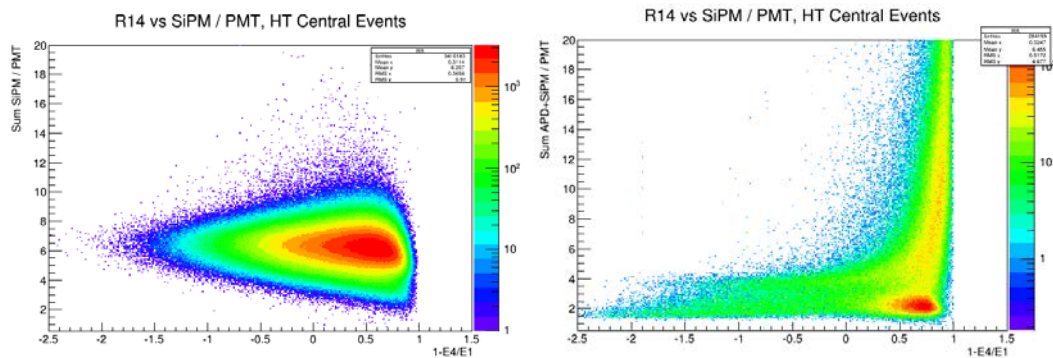


**Figure 11. Ratio SiPM(APD)/PMT vs 1-E4/E1**

Figure 11 gives the ratio of SiPM (APD) Signals to PMT signals versus  $1 - E4/E1$ , where  $E1$  is energy in the central tower and  $E4$  is sum in the four towers adjacent to the trigger tower. Qualitatively, Fig. 11 (right panel) is similar to Fig. 9 (CMS data). About 40% of triggers with APDs are due to NCE-like signals. SiPMs indeed are immune to NCEs. Figure 12 shows the projection of Fig. 11 (left panel), with bands showing  $\pm 5$  sigma cuts. The fraction of anomalous signals with readout based on SiPMs is about  $4 * 10^{-4}$ .

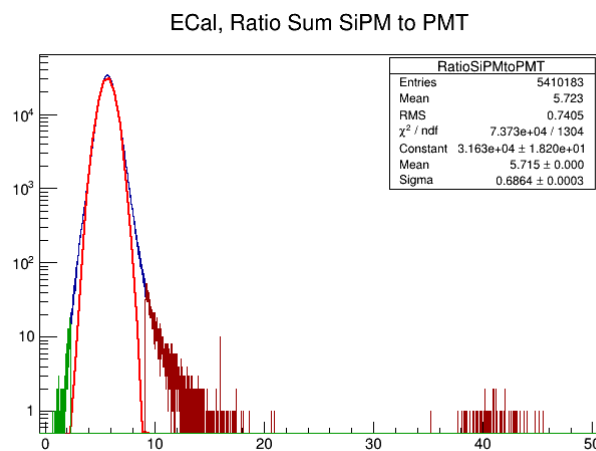


**Figure 12. Fraction of anomalous signals in SiPMs.**

We performed additional tests with the FEMC to investigate how sensitive SiPMs are to environmental conditions in the experiment. We placed a lead converter of  $2X_0$  in length in front of the FEMC in order to emulate a preshower detector. (SiPMs are upstream in the nominal design of FEMC). We performed this test twice, and in both cases we observed an excess in the SiPM signals equivalent to about 90 extra pixels being fired per GeV. The result is shown in Fig. 13 (FitSlicesY of Fig. 10). The orange fit corresponds to lead plate in front of FEMC during the tests. Deviation from linearity at higher energies in both cases is probably due to saturation of the number of fired pixels in the SiPMs.

**This is a large effect.** Ninety extra pixels, which fire due to a converter in front of the FEMC, correspond to 0.4 GeV per GeV in the current FEMC light collection scheme.

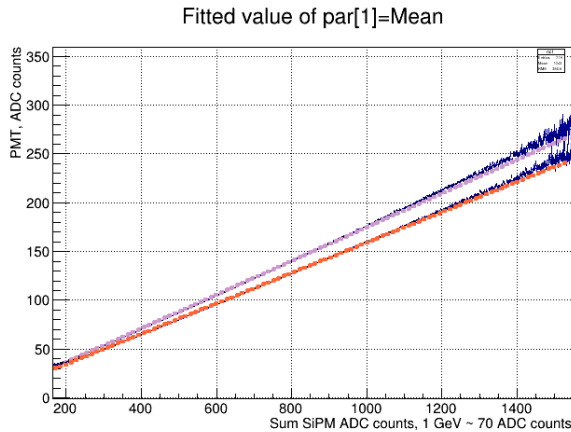


**Figure 13: SiPM vs PMT signals with (orange) and without converter in front of FEMC.**

calorimeter, with one set being blind to scintillation light, and sensitive only to charge particles.

In summary, the first tests with SiPM and APD readouts of the FEMC under realistic collider experimental conditions show that APDs are quite sensitive to NCE and behave similar to what was observed by CMS at LHC. SiPM are much more immune to the NCE, but still could be quite sensitive to environmental conditions, which depend on LY from the detector. It seems now that aiming for very small pixel size, thus increasing number of pixels, and at the same time decreasing the PDE was a mistake, because it could lead to complications in understanding how detector response depends on experimental conditions such as material in front of EMC and variation of radiation and neutron fields in the detector.

The effects that we observed in Run16 at RHIC need to be better quantified because it may affect not only the configuration of the EMC readout, but will require global optimization of the detector, such as choice of absorber for the HCAL section. It is also obvious that the light collection efficiency needs to be improved, but not by simply increasing of the number of sensors per readout channel contrary to what we previously thought and presented to the committee a year ago.

We are currently still taking data with APDs and at this stage it is probably still premature to completely dismiss this option.

## Future Plan

In order to realize EIC calorimeters with the technology we developed over the past a few years we need to solve a few technical issues before we propose to build a large-scale prototype. We expect that about one year from now we may be in a position to start construction of a large scale FEMC prototype, which we then want to operate under realistic collider conditions provided by RHIC. This will mitigate most technical risks for this detector before or at the very first stages of the EIC CD process, and provide a stable platform for development of a complete readout chain for this detector, with all parts being tested under realistic conditions.

The most difficult technical question, it seems now, is to make an efficient and compact light collection scheme. The BEMC, CEMC and FEMC all have different requirements on energy resolution and will operate in different ‘environmental’

There is a concern that the light collection scheme for the PMT (mirror prism) may not be efficient in the corners, and due to a broader shower shape in case with a converter present, the efficiency of light collection on the PMT side may suffer. This we will attempt to clarify with the bench tests during the summer when the setup will be shipped back to UCLA.

Ideally, a test of the sensitivity of SiPMs to ‘shower particles’ should be performed with two identical sets of SiPM readouts located in close proximity on the same side of the

conditions, with the FEMC located in the most challenging place. Configuration of the light collection scheme will depend on behaviour of Si sensors under these conditions.

RHIC provides a unique opportunity to run calorimeter prototypes in conditions close to the EIC. With quite precise estimates on experimental environment conditions we reported previously, we have in hand a ‘controlled’ parasitic experiment. In particular, Run17 (pp) at RHIC is the best opportunity to do that before the next possible run beyond 2022. The beam energy scan runs at RHIC 2019 and 2020 will be very useful, but conditions during these running periods will be quite different from what we expect at EIC, and the interpretation of results may be problematic. Thus, our first priority for next year is to continue studies we started this year by continuing operation of two small EIC prototypes during Run17 placed at the STAR IP. The FEMC prototype needs to be improved to address concerns with light collection on the PMT side. We are proposing to modify the ‘O’ detector in a way similar to the FEMC. These two detectors will be placed at the East side of STAR detector in two different locations and equipped with a better monitoring system than we have now. These prototypes need to be surrounded by a passive lead absorber. Systematic measurements of performance of these two detectors during Run 17 will then guide design of readout schemes for all EIC sampling calorimeters.

Development of a compact and efficient light collection scheme turned out to be a complicated problem. At the beginning we hoped that the SiPMs PDE would improve to reach the ~70% level, thought possible by many when SiPMs started to be widely used. Unfortunately, there was no significant progress in this direction, and a more realistic number for the PDE is probably 25%. It is becoming clear that an optimal scheme to achieve good uniformity and efficiency in light collection will be different for the BEMC, CEMC and FEMC not only because of requirements on energy resolution but due to the ‘mechanical’ constraints each of these detectors will have. As an example, the marginal scheme with a filter between fibers and light guides we developed for the FEMC was subsequently used for the BEMC ‘O’ type detector in 2015, which was one of the reasons leading to degradation of the energy resolution of this detector by about 20%. The readout scheme for each detector has to be optimized differently.

The common problems with light collection for all EIC calorimeters are efficient light collection in the corners of the towers, achieving uniform response across the surface and a large reduction of the surface area due to the small size of SiPMs leading to overall low efficiency. The absolute LYs required for FEMC and CEMC is about 500 p.e./GeV and for BEMC is close to 1000 p.e./GeV. These numbers may change after we complete our studies of sensor behaviour during Run 17. Currently we are about 35% lower than this requirement for the C(F)EMC, due to the ND filter plate placed between the fibers and light guides. Any use of mirrors or reflector compensation with varying reflectivity at the back side of the towers will require an external low Z container for mechanical protection and long term stability. This may work only for the BEMC and FEMC. For the CEMC, the back side of the towers is inaccessible due to mechanical constraints. There are other ways compensation can be achieved without losses due to a ND filter. The most interesting, it seems now, are; 1) is to use a variable sampling frequency and increased diameter of the fibers in the corners of the towers and 2) to use a smaller sensor size but larger number of sensors. Potentially with a larger number of sensors we can find a configuration, which can deliver a uniform response without a ND filter. The other method we tried and reported two years ago is to pre-shrink the output surface of the fibers at the end of the towers; however, at that time we envisioned four separate light guides per tower and for that reason this method was

dropped. A combination of this method and increased number of sensors in a single light guide may work well.

Our second priority for next year is to finalize the light collection scheme for the FEMC and CEMC. Depending on our results, we will then design a light collection scheme for the BEMC. To achieve this goal requires MC simulations and tests in the lab. We don't think that we will be able to carry out a test run at FNAL with the final configuration of the FEMC next year due to our workload with other tasks, but will keep this option open.

## Budget Request

To realize full-scale FEMC prototype we will need to stretch the project for about three years due to budgetary and man power constrains. We present detailed budget request for FY17 and our preliminary estimates for next two years after that are approximately \$200k in FY18 and \$200k in FY19.

Budget for FY17 will cover cost for three iterations of light collection configuration, which require construction of at least three superblocs with different configuration of fibers and sets of readout boards. We would need to expand our DAQ system (which was postponed in previous year due to budget cut) as we'll run continuously one full system at BNL and the other will be in use at UCLA and we need spares. We expect increased travel in FY17 primarily to BNL. For test at BNL we'll need three sets of new SiPM readout for that we request support for IUCF for the electronics development.

SENSL SiPMs	\$5k
Sensor Boards 3 iterations	\$5k
Fibers KURARAY 3 sets	\$12k
Meshes 3 sets	\$3.4k
Tungsten Powder	\$3k
Hamamatsu MPPC 25 um	\$3.25k
Hamamatsu H6559 (spare PMT)	\$1.2k
Hamamatsu C10439 and parts for monitoring system	\$2.7k
CMC080 ADC (spare)	\$4k
FEEs BNL Test 16x3 + spares	\$6k
UCLA Machine and Electronics Shop (26% overhead included)	\$16.1k
UCLA support for students (26% overhead included)	\$15.6k
Travel (26% overhead included)	\$25k
Shipping	\$5k
Mechanical structures for BNL tests	\$6k
Supplies	\$5k
Support for electronics engineer (IUCF) (33% overhead included)	\$26k
Total Direct	\$126.10
Total	\$144.25

**Sub Project Name:** Crystal Calorimeter Development for EIC based on PbWO<sub>4</sub>  
**Project Leader:** Tanja Horn

*High resolution calorimetry is critical at the EIC in the two endcaps for particle identification.* In the electron endcap, particle identification is important for discriminating single photons from, e.g., DVCS and two photons from  $\pi^0$  decay, and e/p. Resolution is essential for particle reconstruction, which is driven by the need to accurately reconstruct the four-momentum of the scattered electrons at small angles. There, the angular information is provided by the tracker, but the momentum (or energy) can come from either the tracker or the electromagnetic calorimeter. The requirements on the inner calorimeter are:

- 1) good *resolution in angle to at least 1 degree*
- 2) *energy resolution to a few %/ $\sqrt{E}$  for measurements of cluster energy*
- 3) *withstand radiation to at least 1 degree with respect to the beam line*

A solution based on PbWO<sub>4</sub> is optimal due to its small Moliere radius.

The critical aspect for *crystal quality, and thus resolution performance* of the EIC inner endcap calorimeter, is the combination of high light output and radiation hardness, which depend strongly on the manufacturing process. Our previous studies have shown that there is significant crystal-to-crystal variation for crystals manufactured by SICCAS. Our results are consistent with observations of crystal-to-crystal variation at PANDA. Examples of such variations are show in Fig. 1. *Evaluation of the variation from crystal to crystal and possibly determining the origin of it is thus one of the main goals of this R&D project.* In the end, this information will be important for what is acceptable for the EIC inner endcap calorimeter. Based on our studies a reasonable batch for such studies consists of at least 10 crystals. Our previous studies also showed significant differences in crystal characterization results at different institutions. *Understanding the effect of such systematic effects is thus important for the interpretation of crystal quality and setting up crystal specifications for EIC, which would be used by a vendor.*

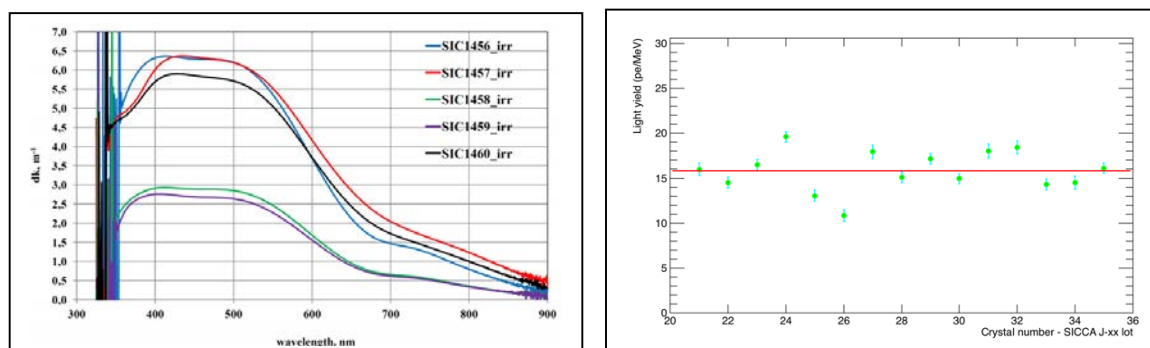


**Fig. 1:** Examples of crystal-to-crystal variation in radiation hardness (left) and light yield (right) observed at PANDA and at CUA/IPNO. None of the 2014 produced SIC crystals would pass the PANDA and JLab NPS requirements of  $dk < 1.1 \text{ m}^{-1}$  after 30 Gy.

### **What was planned for this period?**

- We had planned to finalize setting up the infrastructure for crystal testing, e.g., at IPN-Orsay and CUA, and understand systematic effects in the characterization of 2014 and 2015 SICCAS produced crystals.
- We had planned to procure a reasonable batch of full-sized crystals from Crytur and evaluate their crystal-to-crystal variation.
- We had planned to construct a prototype to study the crystals from either SICCAS or Crytur in test beam and measure the actual energy and position resolution that we could achieve with them. Further, the prototype would have allowed us to test a SiPM-based readout system for the EIC crystal inner calorimeter.

### **What was achieved?**

The *actual* FY16 budget received was 21% of the requested budget.

With these constraints our activities were:

- procurement of *three* full-sized crystals from Crytur
- Work towards finalizing the infrastructure for crystal testing at CUA and IPN-Orsay, and initial studies towards understanding crystal-to-crystal variations and systematic effects
- Results of additional studies at Caltech of radiation damage of a subset of 2014 SIC produced crystals were reported on in our last update.
- Preliminary measurement of light output of one PWO crystal with SiPM

With commitment of internal university and laboratory funds and through synergy with the NPS project at JLab we managed to partially setup crystal testing infrastructure at CUA and IPN-Orsay. Our activities related to crystal characterization were:

- Progress in developing a crystal testing facility at CUA including optical properties and their homogeneity. This is an essential aspect required to quantify the crystal-to-crystal variation of crystals produced at SIC, and thus would provide a measure of the quality that can be achieved by that vendor. As part of the NPS project at JLab a subset of 2014 and 2015 SIC produced crystals has been characterized at CUA. The CUA crystal testing facility benefits from being located in close proximity to Jefferson Lab. This proximity will also be essential

for making progress on understanding systematic effects between different laboratories.

- Since our last report, collaboration with the Vitreous State Laboratory (VSL) enabled detailed characterization of crystals including chemical analysis at CUA, which will be important to understand PbWO<sub>4</sub> crystal-to-crystal variations.
- Since our last report, we also made progress with developing a crystal testing facility at IPN Orsay. This facility is located close to Giessen University and also to the crystal vendor Crytur in the Czech Republic. We have acquired and are commissioning a portable fiber-based spectrometer in order to measure optical transmission longitudinally and transversally to the block axis. This will allow measuring these properties as soon as the crystals are irradiated in the different facilities. The stability of the fiber-based spectrometer has been measured to be better than 0.1% over a 24h period. A mechanical support to hold the fibers and place the block in a reproducible way has been designed and built by the engineering group of IPN-Orsay. Block position and alignment is repeatable to ~0.1 mm. Measurements are underway using old BTCP blocks borrowed from the PANDA collaboration of three new PbWO<sub>4</sub> crystals from Crytur delivered in early 2016. The first results of measurements made possible through collaboration with Giessen University and the JLab NPS project are shown below.

#### **What was not achieved, why not, and what will be done to correct?**

- With the significantly reduced budget we were not able to finalize the crystal testing setups at CUA and IPN-Orsay. However, good progress was made regardless on initial characterization of a subset of SICCAS 2014 crystals and understanding systematic uncertainties due to the setup. There are still open questions on disagreements between measurements of crystal properties at different institutions that have to be addressed. In anticipation of the next phase of crystal testing and with support from the VSL and JLab, we procured some components for a crystal testing facility at CUA. Similarly, IPNO procured components and setup space for crystal testing at Orsay. Assuming that our budget for FY17 will be approved we will complete our crystal testing setup to address the systematic uncertainties between institutions.
- The first Crytur crystal was characterized at CUA. The light yield results are in good agreement with those from Giessen University of the same crystal. INPO procured three full-size crystals from Crytur and made initial measurements in collaboration with Giessen University through the JLab NPS collaboration.

Though the results are encouraging, an evaluation of Crytur crystal-to-crystal variation with a set of three crystals was not possible. Based on our experience this is not sufficient to draw a final conclusion. Assuming that our budget for FY17 will be approved we are planning to obtain a reasonable batch of crystals to evaluate the crystal-to-crystal variation.

- We did not make progress on the prototype studies as we did not obtain funding for FY16 for this activity. Some progress was made in design optimization based on the smaller 3x3 prototype for the NPS at JLab. We also made some progress on exploring prototypes for cooling designs through collaboration with Giessen University. Assuming that our FY17 budget will be approved, we are planning to construct a 5x5 prototype to study the actual energy resolution of the crystals in beam.

**What is planned for the next funding cycle and beyond? How, if at all, is this planning different from the original plan?**

- For the next funding cycle we plan to complete our goals from the FY16 cycle and also try to make progress beyond that. In particular, assuming that we will be approved for funding we will finalize the crystal testing facilities at CUA and IPN-Orsay. In anticipation of the next crystal testing phase and with support from the universities and laboratories, both CUA and IPN-Orsay have been actively procuring components and allocating space. This will allow us to test the optical properties and the homogeneity of crystals produced at SICCAS and procured through synergy with the NPS project at JLab. The results are an essential aspect required to quantify crystal-to-crystal variations and possibly understand their origin, and would thus provide a measure of the quality that can be achieved by that vendor.
- We also plan to procure 10 full-sized crystals from Crytur. This would allow us to do a reliable evaluation of their crystal-to-crystal variation. These crystals could also be tested in the prototype we are planning to build.
- Assuming that our FY16 crystal quality tests are completed successfully and one or two vendors capable of producing such crystals have been identified, the crystal calorimeter R&D will focus in subsequent years on the optimization of geometry, cooling and choices of readout system of the endcap inner crystal calorimeter. Cooling and choice of temperature are important aspects for crystal calorimetry. The choice of temperature balances light output and radiation recovery. Cooling techniques have been explored for the NPS project based on PANDA and CMS. The type of cooling and avoiding condensation depend to

some extend on environmental factors. Our planned future R&D will explore how cooling could be achieved for the inner endcap calorimeter for EIC. Another reason for cooling is the reduction of noise in the readout system. Our initial studies with a SiPM-based readout have shown significant effects of noise at room temperature emphasizing the need for cooling. Our future R&D activities will also explore if cooling is the optimal choice to reduce readout noise and if it is how to implement such a system.

**What are critical issues?**

At this stage, the most critical issues are to complete the FY16 activities. These will address fundamental questions about the crystal-to-crystal variation of crystals procured from SICCAS through synergy with the NPS project, as well as the impact of systematic uncertainties between measurements at different institutions. These also include the evaluation of crystal-to-crystal variation in full-size crystals from SICCAS and Crytur. Further, the construction of a prototype would allow us to study the crystals in test beam and measure the actual energy and position resolution that we could achieve with them. These measurements would provide essential information on crystal specifications and their impact on EIC detector performance.

**Budget Request:**

The original planned timeline and funds requested for our second (third) year R&D in FY16 (FY17) can be found in Section 6 of our July 2015 proposal. In this budget request below, we shifted the budget by one year to fit our current plan taking into account that we received very limited funding in FY2016.

**Table 1** R&D Timeline and Deliverables

Deliverable	FY17 by Quarters				FY18 by Quarters			
	Q1	Q2	Q3	Q4	Q1	Q2	Q3	Q4
Procure crystals from Crytur	X	X						
Crystal quality tests	X	X	X					
Radiation Damage studies	X	X	X					
Construct prototype		X	X					
Test prototype				X	X			
Calorimeter configuration				X	X			
Cooling system studies						X	X	X
Readout system				X	X			
Readout noise reduction						X	X	X

**Table 2.** Funding by task

Item	FY17 (\$K)	FY18 (\$)
Procure crystals from Crytur	40	
Gamma ray radiation studies	5	
Hadron radiation studies	5	
Technical Support	5	15
Parts for prototype	10	
Travel	5	15
Parts for cooling system		40
Parts for readout system		30
<b>Total</b>	<b>70</b>	<b>100</b>

**Table 3.** Funding by Institution

Institution	FY17 (\$K)	FY18 (\$k)
CUA	20	30
JLAB		
BNL	10	20
Caltech	5	
IPN Orsay	35	50
Yerevan		
<b>Total</b>	<b>70</b>	<b>100</b>

## Manpower

*Include a list of the existing manpower and what approximate fraction each has spent on the project. If students and/or postdocs were funded through the R&D, please state where they were located and who supervised their work.*

A list of existing manpower is shown below. All of the participants are supported by external funds and not through the EIC R&D program.

### IPN-Orsay

G. Charles, postdoc  
 F. Georges  
 G. Hull  
 C. Munoz-Camacho

### CUA

M. Carmignotto  
 S. Ali  
 A. Mkrтчhyan, postdoc  
 T. Horn  
 Vitreous State Laboratory

### Yerevan

H. Mkrтчhyan

### BNL

C. Woody  
 S. Stoll

**Caltech**  
R-Y Zhu

## **External Funding**

*Describe what external funding was obtained, if any. The report must clarify what has been accomplished with the EIC R&D funds and what came as a contribution from potential collaborators.*

- All of the FTEs required for working towards finalizing the crystal test setup and crystal characterization are provided by CUA/IPN-Orsay or external grants. The absence of any labour costs makes this proposed R&D effort extremely cost effective.
- The 2014 and 2015 SIC crystals are provided through synergistic activities with independent research for the Neutral Particle Spectrometer (NPS) project at JLab.
- The expertise and use of specialized instruments required for crystal characterization and their chemical analysis, as well as additional crystals samples are made possible through collaboration with the Vitreous State Laboratory (VSL) at CUA that is also collaborating on the NPS project. The VSL has trained and experienced staff and procedures already in place requiring no additional setup overhead beyond what is required for finalizing the crystal test setup, prototype construction, and procuring crystals.

Efforts related to crystal studies as described in the proposal were accomplished with external funds through synergistic activities with the NPS project at JLab. EIC R&D funds were used to procure three Crytur crystals and for parts of the crystal characterization setup at IPN-Orsay and CUA. Additional funds and facilities for crystal characterization were provided by the Vitreous State Laboratory at CUA. Salaries and wages were provided by private external grants from the individual principal investigators, e.g., IPN-Orsay, Yerevan, and the National Science Foundation.

## **Publications**

*Please provide a list of publications coming out of the R&D effort.*

C. Munoz-Camacho et al., “*R&D for high resolution calorimetry at the future Electron-Ion Collider*”, Presentation at the XVIIth International Conference on Calorimetry in Particle Physics, 15-20 May, 2016, Daegu, South Korea

Through synergy with the NPS project at JLab:

T. Horn et al., J.Phys. Conf. Ser. **587** (2015) 1, 012048 “A *PbWO<sub>4</sub>*-based Neutral Particle Spectrometer in Hall C at 12 GeV JLab”

T. Horn et al. “*Physics Opportunities with the Neutral Particle Spectrometer in Hall C*”, presentation at the APS DNP 2015 Fall meeting, Santa Fe, NM

## **APPENDIX:**

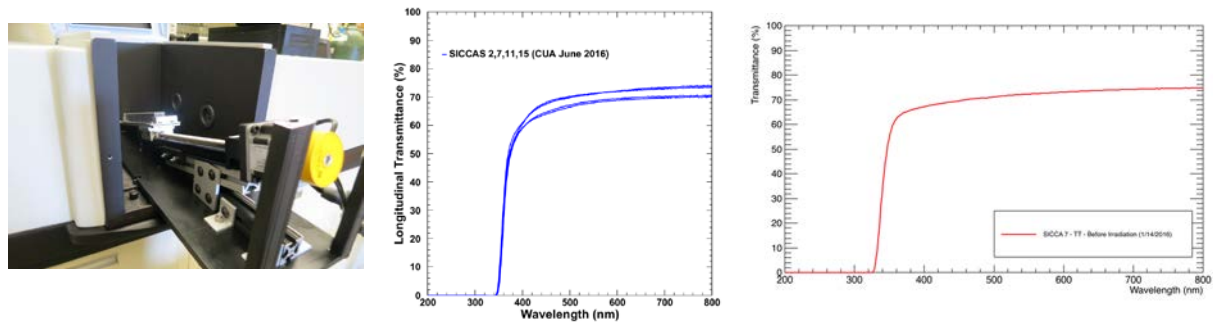
### ***PbWO<sub>4</sub> crystal characterization and initial studies of systematic effects***

At CUA, both longitudinal and transverse transmittance was measured using PerkinElmer Lambda UV/Vis spectrophotometers with double beam, double monochromator, and a large sample compartment. The spectrometers allow for measurements of the transmittance and absorption between wavelengths of 250 to 2500 nm with 1 nm resolution. To measure the 20 cm long crystal samples the spectrometer compartments were modified with a horizontal positioning slide and a programmable stepper motor. The systematic uncertainty in reproducibility of the transmittance measurements is on the order of 0.2%. The light yield was measured with a Photonis XP2262 PMT with a bi-alkali lime glass window. For the light yield measurements a collimated Na-22 source was used to excite the samples. The light yield was measured at a constant temperature of 18°C controlled to better than 1°C. Options for calibrating the PMT for inter-laboratory comparisons are being explored. The systematic uncertainty due to temperature control is better than a few %/°C.

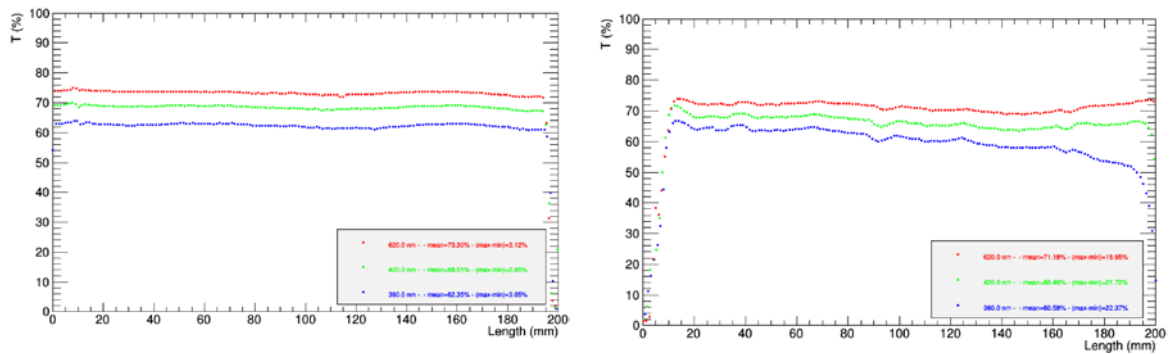
At IPN-Orsay a setup to measure optical transmittance (both longitudinal and transverse) and a setup to measure crystal light yield and timing were commissioned successfully.

Fig. 2 shows longitudinal and transverse transmittance spectra for the most representative set of rectangular PbWO<sub>4</sub> crystals manufactured by SICCAS in 2014 and 2015. Requiring a longitudinal transmittance of greater than 60% at 420 nm as for the JLab NPS project, the three crystals tested in this subset would pass specification. This is consistent with a cross check of the same three crystals carried out at Caltech. A different subset of the same crystal batch that is being characterized at CUA and IPNO was tested at Giessen University through collaboration on the NPS project. The results showed that none of the crystals would pass the required limit. This is consistent with recent observation at PANDA, where only 12% of a recent 2015 produced subset of crystals passed the longitudinal transmittance criterion. The data show a systematic offset between the CUA/Caltech and Giessen University measurements that needs to be understood for interpreting crystal quality and for generating vendor specifications.

A crystal-to-crystal variation in transverse transmittance up to 10% for wavelengths 360 nm, 420 nm, and 620 nm is considered within specifications. Variations in transverse transmittance of more than 15% results in rejection of the crystal sample. Examples of the homogeneity of the transverse transmittance along the crystal length are shown in Fig. 3. For the subset tested thus far, the variation in transverse transmittance is tolerable for most crystals.

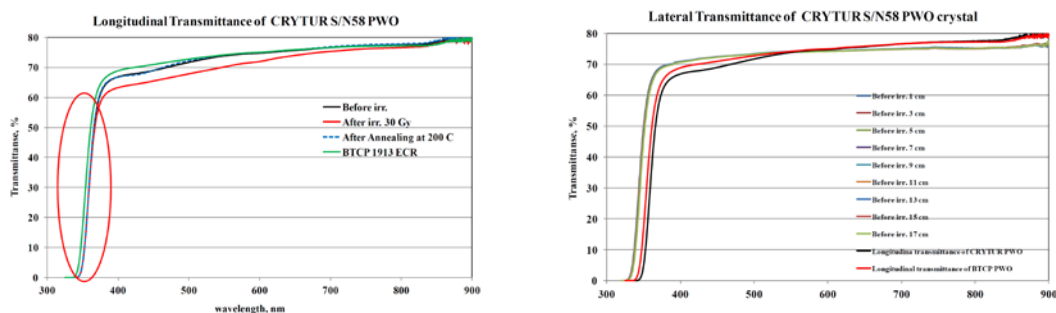


**Fig. 2:** PerkinElmer Lambda750 spectrophotometer with modified sample compartment for transverse transmittance measurements (left), the longitudinal transmittance of a 2014 SIC produced crystal (middle), and the transverse transmittance as a function of position along the crystal of a 2015 SIC produced crystals.



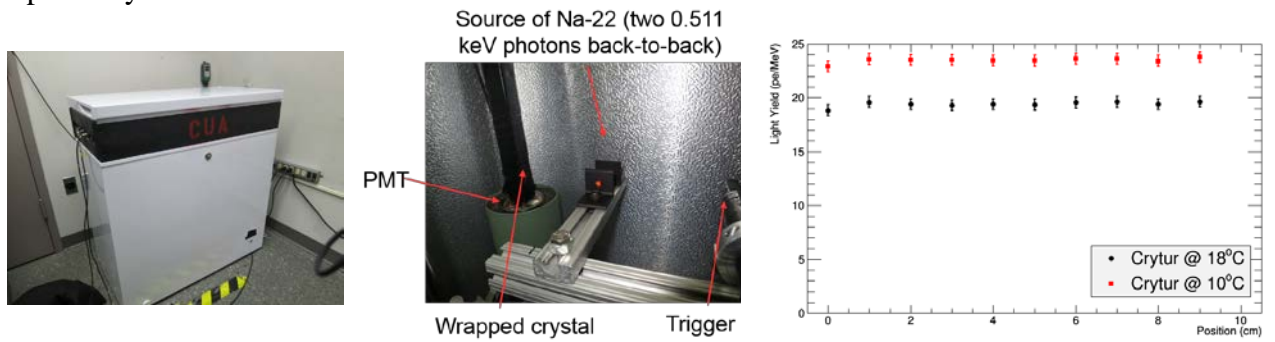
**Fig. 3:** Variation of the transverse transmittance along the crystal for a sample that passes specification (left) and a sample that was rejected (right).

Fig 4 shows longitudinal and transverse transmittance spectra for the most representative set of rectangular PbWO<sub>4</sub> crystals manufactured by CRYTUR in 2015. In general, the values of the longitudinal and transverse transmittance are acceptable. The longitudinal transmittance for this sample does not show an absorption band in the luminescence range of lead tungstate. There is a shift of the fundamental edge of the transmittance relative to a PANDA BTCP crystal (see the ellipse in the longitudinal transmittance spectrum).



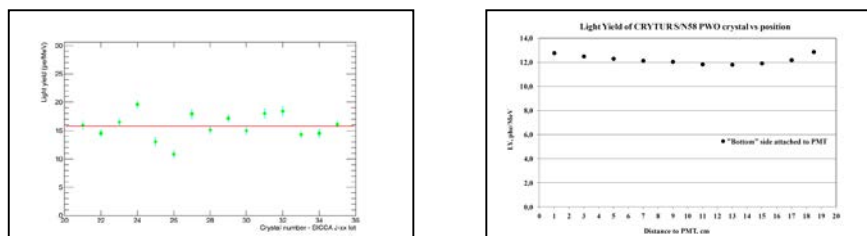
**Fig. 4:** The longitudinal and transverse transmittance of a full-size crystal sample from Crytur in comparison to a BTCP crystal sample. The longitudinal transmittance for this sample does not show an absorption band in the luminescence range of lead tungstate.

Fig. 5 shows the light yield of a 10-cm long CRYTUR crystal compared that we used to cross calibrate our setup at CUA with that at Giessen University. The result of  $19.4 \pm 0.7$  pe/MeV measured at CUA at  $18^\circ\text{C}$  is in good agreement with that from Giessen of  $19.2$  pe/MeV. Note that PMT quantum efficiencies are similar though probably different.



**Fig. 5:** Light yield measurement setup in a temperature controlled dark box (left), with Na-22 source (middle). The result of  $19.4 \pm 0.7$  pe/MeV measured at CUA at  $18^\circ\text{C}$  is in good agreement with that from Giessen of  $19.2$  pe/MeV. The PMT quantum efficiencies are similar though probably different.

For the NPS project the acceptable limit on the light yield at  $18^\circ\text{C}$  is  $15$  pe/MeV. If one applies this criterion to the subset of SICCAS crystals measured, about 55% of the samples will pass the specification limit. This fraction is consistent with a cross check of a subset of the same crystals carried out at Giessen University and another subset of the same crystals carried out at Caltech. In both cases, about 50% of the tested subsets passed specification. The light yield distribution of a subset of 17 crystal samples is shown in Fig. 6 (left). We also tested the light yield of three full-sized Crytur crystals. A representative spectrum is shown in Fig. 6 (right). The light yield is relatively low and would not pass the NPS specifications. The non-uniformity of the light yield along the crystal appears to be tolerable. The low value of the light yield could be due to high doping levels. Lower doping levels will have to be investigated.



**Fig. 6:** Light yield for a subset of crystals produced at SICCAS (left) and Crytur (right) in 2014/15. The variation between crystals is large for SICCAS. The overall light yield is low for Crytur, which could be due to high doping concentrations. The variation of the light yield along the crystal is tolerable.

Another requirement on crystal quality is their performance in a radiation environment. Characterizing the radiation damage on the PbWO<sub>4</sub> crystals is thus another important aspect of this R&D effort. At CUA crystal irradiation options are available through the VSL. These include radioactive sources and an X-ray irradiation system. An initial setup for crystal testing has been constructed and a subset of the 2014 produced SIC crystals and one 2015 Crytur crystal have been tested. This subset of crystals seems to be radiation hard, which is also consistent with our results from Idaho. The rest of the 2014 SICCAS produced crystals and those from 2015 will be tested next once the irradiation setup is complete. Tests of the 2014 SICCAS crystals will be important for understanding differences in crystal characterization results at different institutions. Tests of the 2015 SICCAS and additional Crytur crystals will be essential for understanding crystal-to-crystal variations. At IPN-Orsay through collaboration with the Laboratoire de Chimie Physique at Orsay the group has access to a panoramic irradiation facility based on 3000 Cu Co-60 sources.



**Fig. 7:** Irradiation facility at Orsay housing a strong <sup>60</sup>Co source.

This facility can provide dose rates ranging from 6 to 5000 Gy/h. Thus, high total doses can be accumulated in a short period of time and the effect of different photon irradiation rates can also be studied. In addition, IPN-Orsay houses several beam facilities that can be used to further study the effects of radiation on PbWO<sub>4</sub> blocks. Firstly, a 50 MeV electron facility (ALTO) can provide up to 1 microA of electrons that can complement the irradiation tests made with photon sources. Secondly, a proton (and

several ions) accelerator of the “Van de Graaf” type (Tandem) can provide proton energies in the range of tenths of MeV. This facility is also readily available and will provide information on the crystal damage induced by hadrons, important for the future EIC.

In summary, the test results of SICCAS and Crytur crystals produced in 2014 and 2015 are promising. The optical properties look encouraging though there are aspects that remain to be understood, e.g., low light yield and relatively large crystal-to-crystal variation of the light yield, both essential for high resolution calorimetry in the end caps. The recent Caltech measurements confirm that crystals produced in 2014 are radiation hard. *The next step and key in this R&D effort is to understand the crystal-to-crystal variations and possibly determining their origin. Another important aspect is to understand the differences in crystal characterization results* e.g., between measurements carried out at JLab, Giessen and Caltech. This is important for the interpretation of crystal quality and the setup of crystal specifications for EIC. Data from CUA and IPN-Orsay on the same crystals and calibrated to JLab and Giessen Univ. will help to further understand these systematic effects in the crystal characterization.

### ***Material characterization***

To understand variations in PbWO<sub>4</sub> characteristics like transmittance, light yield, decay times and radiation hardness material characterizations are being carried out at CUA. These include determination of trace element impurities, defects, oxygen vacancies and structural analysis. These studies are being carried out by and in collaboration with the VSL and use a combination of different instruments, e.g., XRF, TEM and SEM, as well as Raman spectroscopy. In particular, XRF analysis is used to identify the crystals’ elemental composition. Non-optimal Pb/W ratios have been shown to be related to poor radiation hardness. The trace element Mo is an impurity in PbWO<sub>4</sub> crystals and can generally be related to slow components. Initial tests of the chemical methods were carried out with a 2-cm long crystal sample produced at SICCAS and a 5-cm long sample from BTCP. The former has a lower optical transmittance than expected even after stimulated and thermal annealing. Chemical analysis showed that the sample consists of two phases and the observed low optical transmittance seems to be due to surface oxidation. Characterization of selected full-size PbWO<sub>4</sub> samples produced by SICCAS in 2014 and 2015 and by Crytur is ongoing.

### ***CRYTUR production and crystal-to-crystal variation***

As of June 2015 Crytur has been able to demonstrate that the company can grow crystals that conform to the strict requirements of PANDA. Since then the company has been focusing on setting up for production, e.g., commissioning new furnaces and polishing machines, and optimizing their capabilities for cutting and polishing crystals. A mechanical holder for cutting of regular prisms was designed, made and tested. It

enables cutting of all sides and small changes of its design also enables cutting of crystal ends. The company was able to reduce the addition for grinding and polishing from 1 to 0.5 mm. The company has also been investing time in the search for new raw materials.

At CUA, we have been characterizing a 10-cm long crystal sample manufactured by Crytur in early 2015. Initial results are shown in Fig. 7. To characterize the crystal-to-crystal variation we have ordered a batch of full-length PbWO<sub>4</sub> crystals. Due to limited funding the batch size was limited to three such crystals. The crystals will be first characterized by IPN-Orsay. Initial results made possible in collaboration with Giessen University through the JLab NPS project of transmittance, light yield and radiation hardness are shown in Figs. 4 and 8.

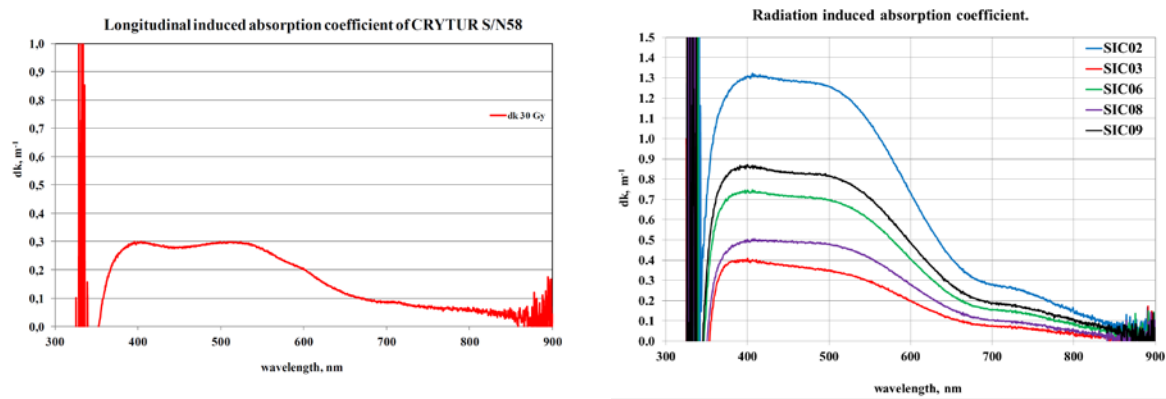


**Fig. 8:** Induced radiation absorption coefficient for a full-sized Crytur crystal produced in 2015 and a subset of 2014/15 produced SICCAS crystals. The Crytur crystal shows a relatively low value of the coefficient in comparison to the SICCAS crystals.

Very good agreement between transmittance measurements of the same crystals has been achieved between Giessen University and IPN-Orsay (Fig. 9), when using the Varian Cary 5000 spectrometer available in Orsay (Fig. 10 – left). Small systematic differences are still observed when using the fiber-based setup illustrated in Fig. 10 (right). However, repeatability of the fiber-based spectrometer is very good, and absolute transmittance measurements can be done by calibrating against the more reliable, but less portable, Varian apparatus.

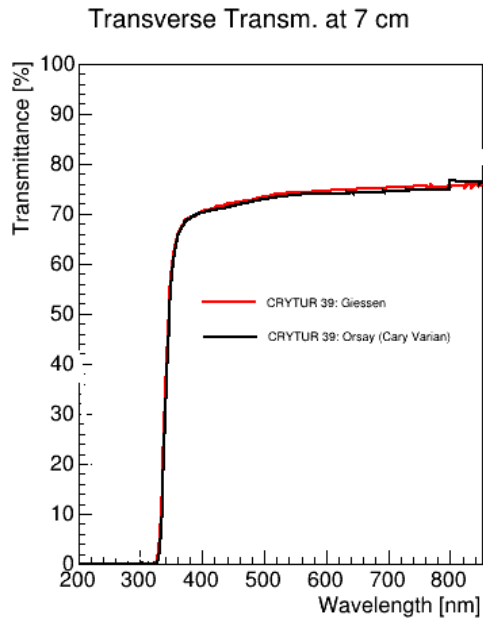


**Fig. 9:** Optical transmittance measured on the same crystal from Crytur by Giessen and IPN-Orsay using the Varian Cary 5000 spectrometer. Excellent agreement is observed between the two independent measurements.

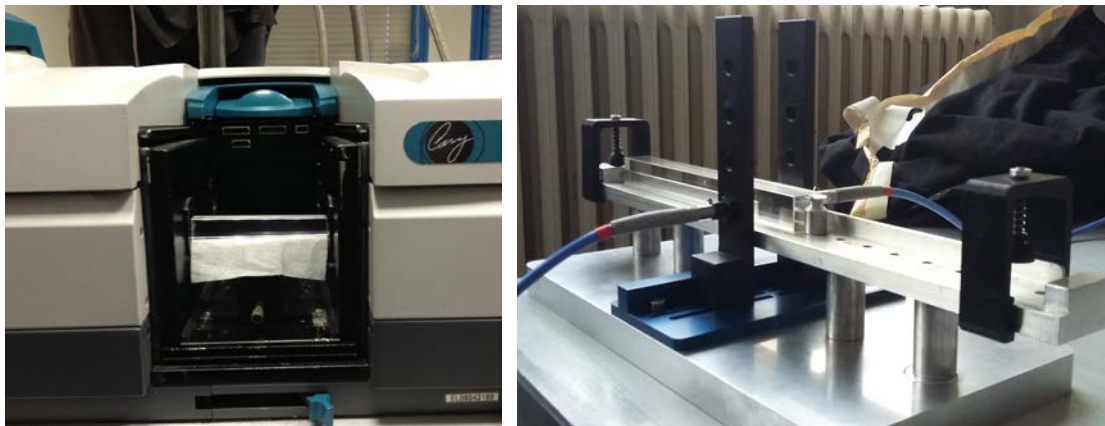


**Fig. 10.** Left: Varian Cary 5000 spectrometer at Orsay for optical transmittance measurements. Right: Fiber-based portable setup for crystal transmittance characterization.

*Though the results are encouraging, this subset of tested crystals is too small to draw a conclusion on crystal-to-crystal variations. The next step in these studies will be to procure a reasonable set of crystals to evaluate these variations.*

#### ***Measurement of light output of PWO crystals with SiPMs***

The light output of SIC crystal #5 was measured using a PMT and with four SiPMs in order to compare the number of photoelectrons detected in both cases. The PMT provided full photocathode coverage of the readout end of the crystal and gave a measure of the total light output. The SiPMs used were Hamamatsu S-12572-015Ps,

which are 3x3 mm<sup>2</sup> devices with 40K 15 μm pixels each. The SiPMs were coupled to the crystal using a 1'' long acrylic light guide which provided ~ 35% light collection efficiency for the 4 SiPMs. The crystal was wrapped in Tyvek paper to improve reflectivity and the light output was measured using cosmic rays traversing the crystal along the 2 cm direction, which gave an energy deposit ~ 20 MeV.

Figure 8 show the pulse height spectrum measured using the PMT. The peak corresponds to ~ 238 photoelectrons and a photoelectron yield of 11.8 p.e./MeV. Figure 9 show the pulse height spectrum measured with the four SiPMs. The peak corresponds to ~ 54 pixels and a photoelectron yield of 2.7 p.e./MeV, which agrees reasonably well with the expected number from the PMT and the light collection efficiency of the light guide. *While this is the first preliminary measurement of the light yield of PWO with SiPMs, and we expect that it can be significantly improved, this level of light yield is sufficient to provide better than 2%/√E in terms of energy resolution.*